JOURNAL OF MOLECULAR SPECTROSCOPY 87, 429–437 (1981)

Far-Infrared Absorption Spectra of $H_2{}^{16}O$, $H_2{}^{17}O$, and $H_2{}^{18}O$

R. H. PARTRIDGE

Division of Electrical Science, National Physical Laboratory, Teddington, Middlesex, TW11 0LW, England

The far-infrared absorption spectra of $H_2{}^{16}O$, $H_2{}^{17}O$, and $H_2{}^{18}O$ have been observed between 10 and 47 cm^{-1} at resolutions up to 0.015 cm^{-1} and path lengths up to 13 m. A number of weak absorption lines have been directly observed for the first time, including some from all three species in the (010) vibrational state. Line positions have been measured to a standard deviation of 0.0006 cm^{-1}.

INTRODUCTION

The increasing amount of work concerned with propagation of radiation through the atmosphere makes study of absorption by the water molecule a topic of continuing interest. Such propagation in the stratospheric region, especially in connection with measurement of chemical pollutants at these high altitudes and relatively low pressures, makes it necessary to measure with increasing accuracy the positions of the rotational lines of water in its various stable isotopic forms.

The measurements described here are of the far-infrared absorption of gaseous $H_2{}^{16}O$, $H_2{}^{17}O$, and $H_2{}^{18}O$ between 10 and 47 cm^{-1}. By using considerably higher resolution and longer sample path lengths than in the last major study (*1*) of $H_2{}^{16}O$ and $H_2{}^{18}O$ in this spectral region it was possible to measure line positions to greater accuracy and to observe a number of weak lines not seen previously. There does not appear to have been a previous study of $H_2{}^{17}O$ in this region by broad band techniques. Using resolutions up to 0.015 cm^{-1} and path lengths up to 13 m it was possible to determine line positions for more than 50 lines with an average standard deviation of about 0.0006 cm^{-1}.

EXPERIMENTAL DETAILS

Spectra were measured with a phase modulated NPL–Grubb Parsons Cube interferometer modified to take an inclined mirror moving mirror arm (*2*) or a cube corner moving mirror arm (*3*). The former mirror drive system was used for the earlier measurements but mechanical problems with the drive mechanism forced its abandonment. In the latter moving mirror system radiation from the beam splitter is directed into the bottom half of a 5-in aperture hollow cube corner mirror fixed onto a moving carriage and leaves it from the top half to meet a fixed plane mirror at normal incidence which exactly reverses its direction. This combination of mirrors has the advantage that the direction of the radiation returned to the beam splitter is independent of any tilting of the cube corner during its travel, thus re-

0022-2852/81/060429-09$02.00/0

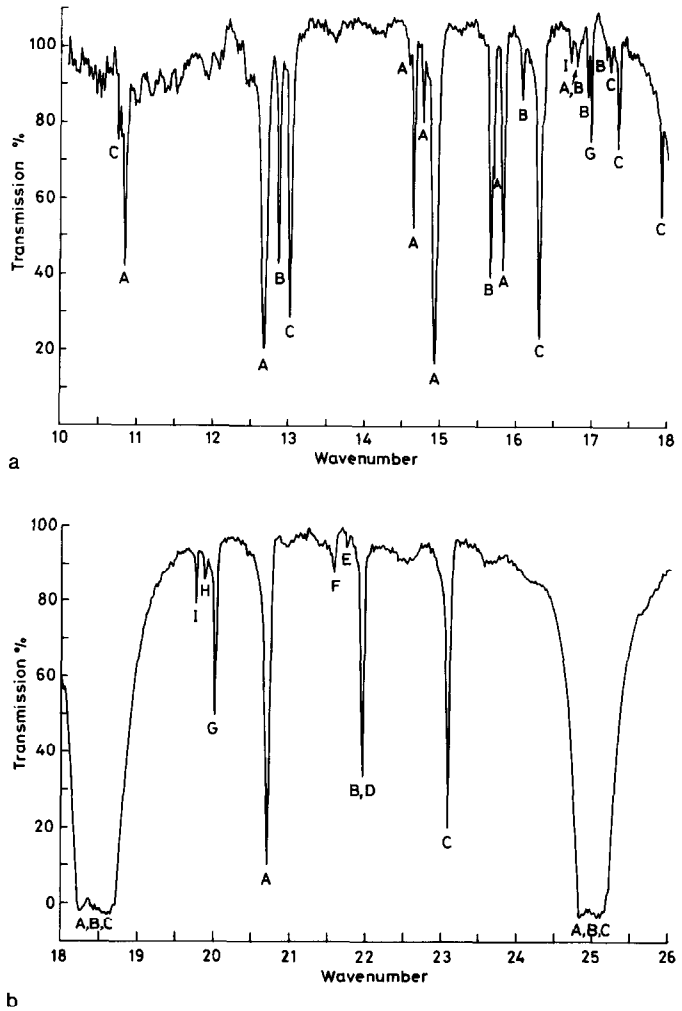

FIG. 1. Isotopically enriched water vapor. Pressure 10 Torr, path length 13 m. Resolution (apodized) 0.025 cm^{-1}. Line identifications are: A: $H_2{}^{16}O$, B: $H_2{}^{17}O$, C: $H_2{}^{18}O$, D: $H_2{}^{16}O$ (010), E: $H_2{}^{17}O$ (010), F: $H_2{}^{18}O$ (010), G: $HD^{16}O$, H: $HD^{17}O$, I: $HD^{18}O$.

moving one prime source of interferometer error. The cube corner was mounted on a Unimatic linear table driven by a stepper motor. The drive had a linear movement of 125 mm which, due to the double pass through the cube corner, gave a maximum optical path variation of 0.5 m.

The source was a medium-pressure mercury lamp type HPK-125 driven by a current stabilised power supply and the detector a QMC Instruments InSb hot-electron detector mounted in a helium cryostat of such capacity as to allow continuous measurements for at least 30 h.

The sample cell was either a 0.8 m brass tube with TPX end windows, for study of the strongest water lines, or else a 1 m modified White cell (*4*) fed by a

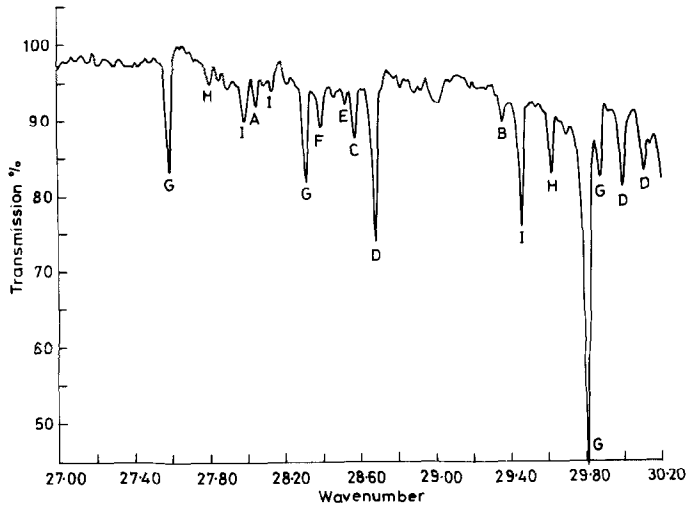

c

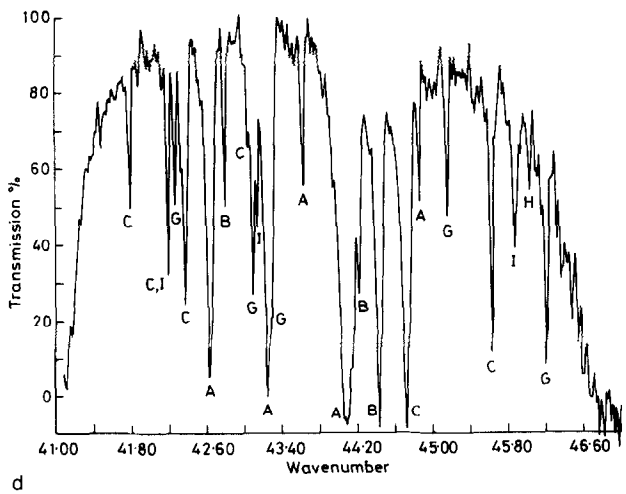

d

FIG. 1—*Continued.*

600 mm focal length TPX lens. Tests showed that there was some ambiguity in the optical path lengths obtained in the White cell since whereas visible light images of the mercury lamp formed on the single mirror were well separated from each other the far-infrared images were clearly being much broadened by diffraction and overlapping of the infrared reflection orders could easily occur. Thus whilst up to 8 passes along the cell were fairly unambiguous, attempts to use more than 12 such passes gave rise to a spread of path lengths together with a radiation loss that increased appreciably with increasing wavelength.

The water samples used were either natural water or an isotopically enriched mixture containing approximately 74% $H_2{}^{16}O$, 10% $H_2{}^{17}O$, and 16% $H_2{}^{18}O$ plus

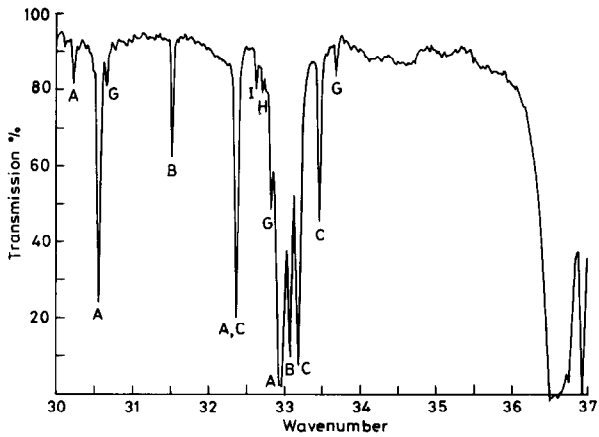

FIG. 2. As for Fig. 1 but pressure 3.3 Torr and resolution (apodized) 0.029 cm^{-1}.

traces of the three mono-deuterated species. Eleven interferograms were run with these samples using pressures between 1 and 16 Torr and path lengths between 0.8 and 13 m. The runs each lasted 20 to 30 h using a time constant of 1 to 3 sec and generated up to 7500 data points for an optical path difference of 350 to 480 mm; the longest run times and time constants were used for the longest sample path lengths to compensate for radiation losses in the White cell. The cell pressure was monitored continuously with a Baratron gauge.

The sample interferograms were Fourier transformed, interpolated by a factor of 4 to give better definition of the absorption lines and then ratioed against similar spectra taken in the absence of a sample to yield a true transmission spectrum. The positions of all peaks above a specified size were automatically measured by a peakfinder procedure immediately after the ratioing, with each peak maximum being determined by fitting a quadratic function to the three main spectral points of each peak. Values from peaks with transmissions less than 10% or greater than

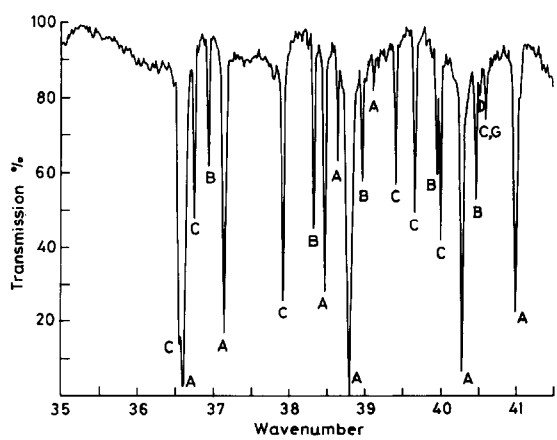

FIG. 3. As for Fig. 1 but pressure 1.1 Torr, path length 5 m and resolution (apodized) 0.022 cm^{-1}.

TABLE I

$H_2{}^{16}O$ Line Positions and Assignments

Assignment	S_{rel}	Observed	Ref 9	Ref 16	Ref 13
(000) state					
$8_{63} \leftarrow 7_{70}$	3.3 - 4	16.7990	16.7985		
$10_{56} \leftarrow 11_{29}$	2.0 - 4	28.054	28.0533		
$9_{28} \leftarrow 8_{35}$	3.7 - 3	30.2294	30.2278		
$4_{22} \leftarrow 3_{31}$	1.8 - 1	30.5605	30.5599		
$5_{24} \leftarrow 4_{31}$	1.8 - 1	32.3664	32.3663		
$2_{02} \leftarrow 1_{11}$	3.1	32.9539	32.9539	32.9554	
$3_{12} \leftarrow 3_{03}$	20	36.6036	36.6037	36.6056	
$1_{11} \leftarrow 0_{00}$	6.1	37.1373	37.1369	37.1371	
$7_{25} \leftarrow 8_{18}$	1.5 - 2	38.248	38.2469		
$3_{12} \leftarrow 2_{21}$	3.2	38.4648	38.4632	38.4661	
$6_{34} \leftarrow 5_{41}$	2.6 - 1	38.6383	38.6380	38.6378	
$3_{21} \leftarrow 3_{12}$	21	38.7909	38.7909	38.7905	
$7_{44} \leftarrow 6_{51}$	2.2 - 2	39.1125	39.1121		
$4_{22} \leftarrow 4_{13}$	6.6	40.2829	40.2823	40.2827	
$2_{20} \leftarrow 2_{11}$	5.8	40.9881	40.9880	40.9894	
$7_{43} \leftarrow 6_{52}$	8.5 - 2	42.6383	42.6385		
$8_{27} \leftarrow 7_{34}$	8.1 - 2	43.2452	43.2435		
$8_{45} \leftarrow 9_{18}$	6.2 - 3	43.6296	43.6290		
$6_{25} \leftarrow 5_{32}$	6.4 - 1	44.1001	44.0995	44.0996	
$7_{44} \leftarrow 8_{17}$	3.6 - 3	44.858	44.8532		
$5_{23} \leftarrow 5_{14}$	16	47.055	47.0532	47.0548	
(010) state					
$1_{10} \leftarrow 1_{01}$	3.7 - 3	21.9488			21.9488
$2_{11} \leftarrow 2_{02}$	2.2 - 3	28.6858			28.6818
$2_{02} \leftarrow 1_{11}$	1.1 - 3	29.9993			30.0011
$3_{12} \leftarrow 2_{21}$	8.8 - 4	30.1098			30.1063
$3_{12} \leftarrow 3_{03}$	1.0 - 2	40.518			40.5152

80% were discarded (or, for the very weakest lines, quoted with reduced accuracy), the latter as being too much affected by noise and the former as coming from peaks too broadened for accurate measurement. Each transformed interferogram was individually calibrated by reference to at least six lines of $H_2{}^{16}O$, $H_2{}^{17}O$, $H_2{}^{18}O$ whose wavenumbers are very accurately known from measurements using microwave techniques (*5–8*) different such lines being used for different runs depending on the prevailing conditions of sample pressure and path length. The set of observed line positions could usually be fitted to their microwave technique values with a standard deviation of less than 0.0005 cm^{-1}. The observed wavenumber values given here for each line are averages of values from in most cases at least four different runs and the average standard deviation for such sets of run values was 0.0006 cm^{-1}.

TABLE II

$H_2{}^{17}O$ Line Positions and Assignments

Assignments	S_{rel}	Observed	Ref 6	Ref 10	Ref 14	Ref 16
(000) state						
$6_{43} \leftarrow 5_{50}$	1.0 - 2	16.0814	16.080	16.0869		16.093
$5_{33} \leftarrow 4_{40}$	1.5 - 2	16.9422	16.942	16.9441	16.920	16.963
$6_{42} \leftarrow 5_{51}$	3.8 - 3	17.193	17.190	17.1992		
$5_{32} \leftarrow 4_{41}$	7.5 - 2	21.963	21.965	21.9682	21.945	21.976
$9_{28} \leftarrow 8_{35}$	3.6 - 3	29.363	29.351			
$4_{22} \leftarrow 3_{31}$	1.9 - 1	31.5172	31.517	31.5171	31.498	31.539
$2_{02} \leftarrow 1_{11}$	3.1	33.0747	33.073	33.0736	33.070	33.076
$1_{11} \leftarrow 0_{00}$	6.1	36.9312	36.931	36.9311	36.940	36.930
$3_{21} \leftarrow 3_{12}$	21	38.3267	38.325	38.3257	38.328	38.305
$3_{12} \leftarrow 2_{21}$	3.3	38.9674	38.965	38.9649	38.966	38.964
$4_{22} \leftarrow 4_{13}$	6.5	39.9477	39.948	39.9481	39.952	39.945
$2_{20} \leftarrow 2_{11}$	5.7	40.4615	40.460	40.4606	40.452	40.455
$7_{43} \leftarrow 6_{52}$	9.3 - 2	44.217	44.197	44.2159		44.220
$6_{25} \leftarrow 5_{32}$	6.5 - 1	44.4360	44.436	44.4294	44.422	44.433
$5_{23} \leftarrow 5_{14}$	16	46.9171	46.915	46.9144	46.913	46.890
(010) state						
$1_{10} \leftarrow 1_{01}$	3.7 - 3	21.759				
$2_{11} \leftarrow 2_{02}$	2.2 - 3	28.531				

RESULTS

The assignment of lines in the various spectra was done by use of the rotational energy tables prepared for $H_2{}^{16}O$ by Flaud *et al.* (*9*) and for $H_2{}^{17}O$ and $H_2{}^{18}O$ by Helminger and DeLucia (*10*), which used data from microwave and mid-infrared experiments. Relative line intensities were often useful in making definite assignment and these were calculated from the relation

$$S_{rel} = \{\mathrm{Exp}[-E_u/kt] - \mathrm{Exp}[-E_l/kT]\}\tilde{\nu}_{ul}S_{ul}g_l,$$

where E_u, E_l are the upper and lower state energies respectively, $\tilde{\nu}_{ul}$ is the transition wavenumber, S_{ul} the transition strength (*11*), g_l the lower state statistical weight and the temperature T was taken as 300 K.

Absorption lines of the mono-deuterated species $HD^{16}O$, $HD^{17}O$, and $HD^{18}O$ were also found to be present and these were assigned in a similar way using rotational energy levels from Benedict and Clough (*12*) for $HD^{16}O$ and from Steenbeckeliers and Bellet (*12*) for $HD^{18}O$. As no similar $HD^{17}O$ levels seem to exist the necessary transitions were calculated by use of the observed $HD^{16}O$/$HD^{18}O$ values together with the empirical Fraley–Rao interpolation rule (*10*) which states in its simplest form that

TABLE III

$H_2{}^{18}O$ Line Positions and Assignments

Assignments	S_{rel}	Observed	Ref 1	Ref 10	Ref 14	Ref 16
(000) state						
$9_{28} \leftarrow 8_{35}$	3.4 - 3	28.5812			28.580	28.569
$2_{02} \leftarrow 1_{11}$	3.1	33.1784		33.1789	33.178	33.191
$5_{24} \leftarrow 4_{31}$	2.0 - 1	33.4663		33.4656	33.467	33.468
$3_{12} \leftarrow 3_{03}$	20	36.5477		36.5463	36.546	36.544
$1_{11} \leftarrow 0_{00}$	6.0	36.7490	36.7450	36.7487	36.750	36.720
$3_{21} \leftarrow 3_{12}$	21	37.9171	37.9127	37.9163	37.916	37.923
$3_{12} \leftarrow 2_{21}$	3.3	39.4080	39.4083	39.4073	39.407	39.412
$4_{22} \leftarrow 4_{13}$	6.4	39.6574	39.6518	39.6562	39.658	39.657
$2_{20} \leftarrow 2_{11}$	5.6	39.9950	39.9945	39.9945	39.996	39.995
$7_{44} \leftarrow 6_{51}$	2.6 - 2	41.7828		41.7794	41.785	41.731
$8_{27} \leftarrow 7_{34}$	7.9 - 2	42.367		42.3651	42.362	42.368
$6_{25} \leftarrow 5_{32}$	6.7 - 1	44.7230		44.7221	44.723	44.721
$7_{43} \leftarrow 6_{52}$	1.0 - 1	45.6255		45.6217	45.624	45.618
$5_{23} \leftarrow 5_{14}$	16	46.8003		46.7979	46.798	46.793
(010) state						
$1_{10} \leftarrow 1_{01}$	3.7 - 3	21.588				
$2_{11} \leftarrow 2_{02}$	2.2 - 3	28.400				

$$\frac{\tilde{\nu}_{17} - \tilde{\nu}_{16}}{\tilde{\nu}_{18} - \tilde{\nu}_{16}} \simeq 0.53,$$

where $\tilde{\nu}_{16}$, $\tilde{\nu}_{17}$, and $\tilde{\nu}_{18}$ are the transition wavenumbers of similar transitions in water molecules that differ only in their oxygen mass numbers.

Some lines of $H_2{}^{16}O$ excited to the (010) vibrational state were also identified, using rotational energies derived from the study of near-infrared flame spectra by Camy-Peyret *et al.* (*13*). The ν_2 bending vibration wavenumber is 1595 cm^{-1} and thus at 290 K less than 0.04% of the water molecules will be in this vibrational state. Rotational energy levels for the (010) states of $H_2{}^{17}O$ and $H_2{}^{18}O$ are not currently available. However, tentative assignments for the $1_{10} \leftarrow 1_{01}$ and $2_{11} \leftarrow 2_{02}$ transitions of these were made here (Tables II and III), although the lines involved (see Figs. 1b and c) are very weak even at the highest pressures and sample path lengths used. These assignments were made on the basis that the lines lie in the vicinity of the corresponding $H_2{}^{16}O$ lines, that their Fraley–Rao ratios are very reasonable with values of 0.53 for the 21-cm^{-1} lines and 0.54 for the 28-cm^{-1} lines and that the intensities of each $H_2{}^{16}O/H_2{}^{17}O/H_2{}^{18}O$ triplet of lines are approximately in the ratio of the abundances of these species.

The far-infrared absorption spectrum of water vapor under comparatively low absorption conditions is well known (see, for instance, (*1*)). By contrast Fig. 1

shows portions of the transmission spectrum of the isotopically enriched water vapor sample at one of the highest pressure and path length combinations used here. Since the intervening portions are largely blacked out under these conditions by a series of strong absorption lines they are shown in Figs. 2 and 3 as from two different runs at lower pressures and path lengths. All the spectra shown have been apodized with a linear weighting function in order to achieve greater visual clarity by reducing the higher noise frequencies, but wavenumber measurements were found to be slightly more accurate when made on unapodized spectra. Since most interferograms were run until the signal was comparable with the noise level the sidelobes of the main absorption lines were generally too small to need suppression by apodization. The higher noise level seen in Fig. 1d is caused by the rapidly falling sensitivity of the hot electron detector at shorter wavelengths.

Tables I to III give the wavenumbers of the observed lines of $H_2{}^{16}O$, $H_2{}^{17}O$ and $H_2{}^{18}O$ in the ground and (010) vibrationally excited states. Values given to three rather than four decimal places indicate lower precision due to overlapping lines or very weak absorption. The wavenumbers are compared where possible with other recent transition wavenumbers, mostly derived from a combination of mid-infrared and microwave data. No values are given for lines previously measured by microwave techniques since these were used to standardise the observed values.

Good agreement is seen in Table I between the observed values for $H_2{}^{16}O$ in the ground vibrational state and those derived from the rotational energy levels of Flaud *et al.* (*9*), with the average difference between them (for line values given to four decimal places) being 0.0005 cm^{-1}. Agreement for the (010) state of $H_2{}^{16}O$ is not quite so good for three of the four most accurately measured lines, with differences between the observed values and those derived from the study of Camy-Peyret *et al.* (*13*) being several times greater than the standard deviation of the observed values from different runs.

For $H_2{}^{17}O$ the data of DeLucia and Helminger agree best with the values observed here, with their earlier data (*6*) fitting marginally better than their later data (*10*), while for $H_2{}^{18}O$ transition energies derived from the sets of energy levels in (*10*, *14*) agree about equally well with the observed values.

ACKNOWLEDGMENTS

I am most grateful to Dr. J. W. Fleming for many discussions and for the use of apparatus and computer programs, and likewise to Mr. G. K. J. Gibson for much technical assistance. Valuable contributions were also made by Mr. M. Gifford and Miss C. Deely.

RECEIVED: October 2, 1980

REFERENCES

1. J. W. FLEMING AND M. J. GIBSON, *J. Mol. Spectrosc.* **62,** 326–337 (1976).
2. R. H. PARTRIDGE, *Infrared Phys.* **19,** 571–574 (1979).
3. Designed by Dr. J. W. Fleming (unpublished).
4. H. J. BERSTEIN AND G. HERTZBERG, *J. Chem. Phys.* **16,** 30–39 (1948).
5. F. C. DELUCIA, P. HELMINGER, R. L. COOK, AND W. GORDY, *Phys. Rev. A* **5,** 487–490 (1972).

6. F. C. DeLucia and P. Helminger, *J. Mol. Spectrosc.* **56,** 138–145 (1975).
7. F. C. DeLucia, P. Helminger, R. L. Cook, and W. Gordy, *Phys. Rev. A* **6,** 1324–1326 (1972).
8. F. C. DeLucia, R. L. Cook, P. Helminger, and W. Gordy, *J. Chem. Phys.* **55,** 5334–5339 (1971).
9. J. M. Flaud, C. Camy-Peyret, and J. P. Maillard, *Mol. Phys.* **32,** 499–521 (1976).
10. P. Helminger and F. C. DeLucia, *J. Mol. Spectrosc.* **70,** 263–269 (1978).
11. C. H. Townes and A. L. Schawlow, "Microwave Spectroscopy," Appendix V, McGraw-Hill, New York, 1955.
12. Communication from Dr. G. Steenbeckeliers to Dr. J. W. Fleming.
13. C. Camy-Peyret, J. M. Flaud, J. P. Maillard, and G. Guelachvili, *Mol. Phys.* **33,** 1641–1650 (1977).
14. R. A. Toth, J. M. Flaud, and C. Camy-Peyret, *J. Mol. Spectrosc.* **67,** 185–205 (1977).
15. J. Kauppinen, T. Karkkainen, and E. Kyro, *J. Mol. Spectrosc.* **71,** 15–44 (1978).
16. F. Winther, *J. Mol. Spectrosc.* **65,** 405–419 (1977).